S. K. FRIEDLANDER[1] and H. F. JOHNSTONE
University of Illinois, Urbana, Ill.

Deposition of Suspended Particles from Turbulent Gas Streams

Rate of particle transfer is always less than or equal to the transfer rate of the common gases which follow approximately the Reynolds analogy

When a stream of gas carrying suspended particles flows in turbulent motion past a surface, the particles are deposited because of the radial fluctuating component of velocity. The transport of suspended particles by turbulent streams of water has been studied by Kalinske and van Driest (*5*) and by Vanoni and Hsu (*12*). The mixing and distribution of liquid droplets in high velocity gas streams were studied by Longwell and Weiss (*10*). Only a few experiments have been reported on the important problem of deposition of droplets (*7*) and the formation of deposits of dust (*11*) from turbulent gas streams. An experimental study of the rate of deposition of dust particles on the walls of tubes is reported here with an analysis of the mechanism of transport of particles in a turbulent stream. The net rate of deposition depends on both the rate of transport of the particles to the wall and the rate of re-entrainment; the second effect was reduced to a minimum by allowing only a single layer of particles to accumulate on the surface and taking precautions to ensure adherence of all particles that struck the wall.

Equipment and Methods

In these experiments (*2*) three types of powders were used: two grades of iron powder (Antara Chemicals Division, General Dyestuff Corp.) with mass median diameters of approximately 3 and 5 microns, respectively, and a standard geometric deviation of about 1.4 (*7*); an aluminum powder of approximately 5-micron mean diameter (Reynolds Metal Co.); and lycopodium spores (McKesson and Robbins Co.), which according to Gregory have a diameter of about 30 microns (*4*).

The general arrangement of the apparatus is shown in Figure 1. The powders were dispersed by an atomizing nozzle made of glass with a throat 16 mm. long and 3 mm. in inner diameter. The compressed air used for the nozzle was passed first through a glass fiber filter and then through a pressure-regulating valve. Before entering the observation tube, the aerosol passed through a 5-gallon drum fitted with a mixing baffle at the inlet. The aerosol stream from the nozzle was mixed with a secondary stream of air to adjust the desired flow rate. The aerosol was drawn through the system by a rotary positive vacuum pump.

The observation tubes were made of either glass or brass. The dimensions are shown in Table I. The smaller glass tubes were thin-walled borosilicate glass. The observation regions were made by grinding the wall and polishing the flat surface with a suspension of No. 150 Carborundum powder in oil and a flat brass strip. The observation sections for the brass tubes were made by cutting out sections 3 inches long and replacing them with new pieces of the tubes machined to fit.

A glycerol jelly adhesive described by Gregory (*4*) and "pressure-sensitive" Scotch tape (with adhesive on both sides) were used in some runs to prevent re-entrainment of the particles.

Type HA Millipore filters (Lovell Chemical Co.) were used to determine the concentrations of the iron and aluminum aerosols. Isokinetic flow through the sampling tube was obtained by using a tapered brass probe with a tip of the proper size. The probe was inserted through a tee section into the top of the observation tube, so that the gas did not make any turns on the way to the filter. A rotary pressure and vacuum pump was used for sampling the aerosol.

Concentrations of the iron and aluminum particles were determined by counting at least 100 particles on a known area of the filter after filtering measured volumes of gas. The concentrations, while measured at the axes of the tubes, were assumed to be the averages for the stream, as the fraction of particles removed was small and large concentration

Table I. Dimensions of Observation Tubes

Material	Diameter (D), Cm.	Distance from Inlet to Observation Region (L_t), Cm.	L_t/D	Total Length, Cm.
Glass	0.54	24	44.5	33
	0.58	Entrance region tube		
	1.305	42	32.2	60
	2.50	89	35.5	118
Brass	1.38	48 and 74	34.8 and 53.7	91.5
	2.50	65	26	109

[1] Present address, Department of Chemical Engineering, Columbia University, New York, N. Y.

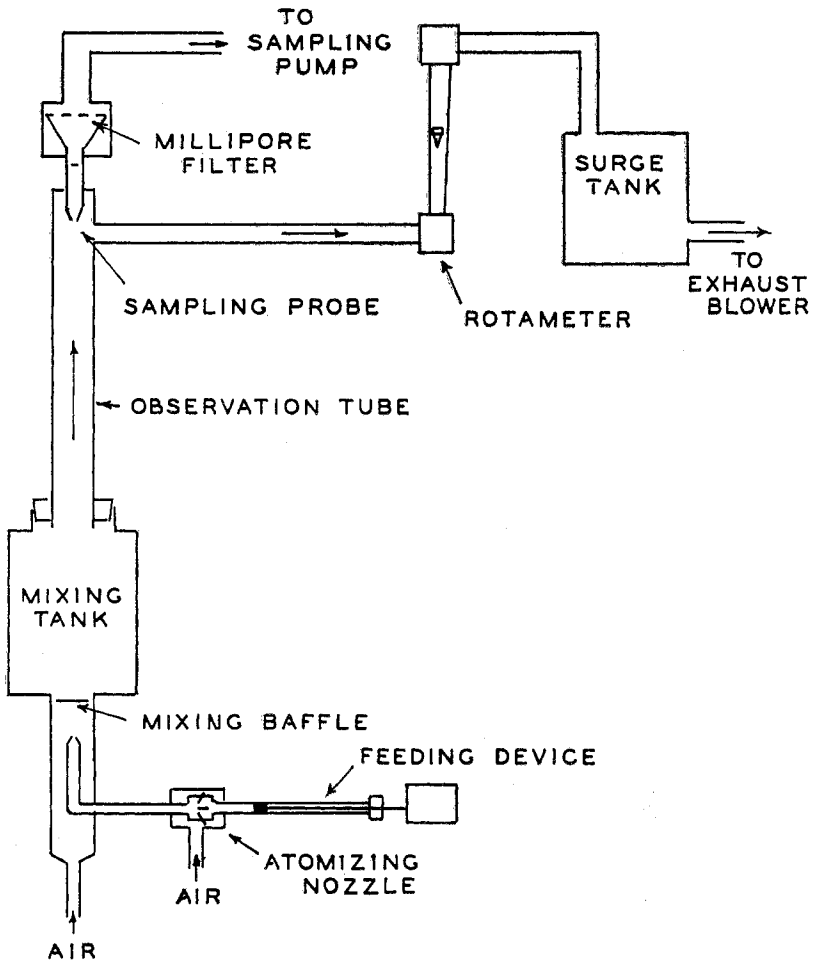

Dust particle deposition rate was studied in this apparatus

gradients did not exist. The particle size ranges used in determining the concentrations were the same as those used in counting the number of particles in the deposits.

Before each run, the section of the duct on which the deposition was to be observed was cleaned carefully. For the 0.54- and 1.3-cm. glass tubes, a hot solution of detergent in demineralized water was used. The amount of deposition in the brass tubes and in the 2.5-cm. glass tube was obtained in one of three ways: In some cases, the wall was cleaned initially by applying a piece of Scotch tape and stripping it off, and at the end of the run the deposit was removed in the same way with another piece of tape and the particles were counted under a microscope; in other runs, a piece of pressure-sensitive tape was applied to the test section before starting and removed at the end of the run, and the number of particles deposited were counted; in the studies with lycopodium powder, glycerol jelly was applied to the section which was removed at the end of the run and the particles were counted under a microscope. The rate of deposition in the 0.54- and 1.3-cm. glass tubes was observed by counting the particles on impact with the wall.

In general, the duration of the runs was between 5 and 30 minutes. When the particles were deposited too rapidly, or the deposition rate was inconveniently slow, the run was repeated with a different concentration of aerosol particles. The concentration was controlled by adjusting the amount of powder fed to the atomizing nozzle or by using only a fraction of the powder injected by the nozzle.

The iron and aluminum particles were counted under a microscope with a 95 × objective and a 15 × eyepiece. A calibrated Porton "globe-and-circle" graticule was used for measuring the particle size. In the runs with lycopodium powder, the concentration of the spores was determined by passing a sample of gas stream through a glass fiber filter which was weighed before and after each run and multiplying the weight increase by 9.39×10^7, the number of particles per gram found by Gregory (*4*). Preliminary tests with the Millipore filters showed that only a few agglomerates were present and all particles were nearly the same size.

The deposition rate was determined by counting at least 100 particles deposited on a known area of tube wall in a measured interval of time. At the beginning of the work, before the effect of the particle size on transfer rate was recognized, particles were counted from a range of sizes and a simple arithmetic average was taken. For the later runs, only the particles in a narrow size range were counted. Table II shows the particle sizes used.

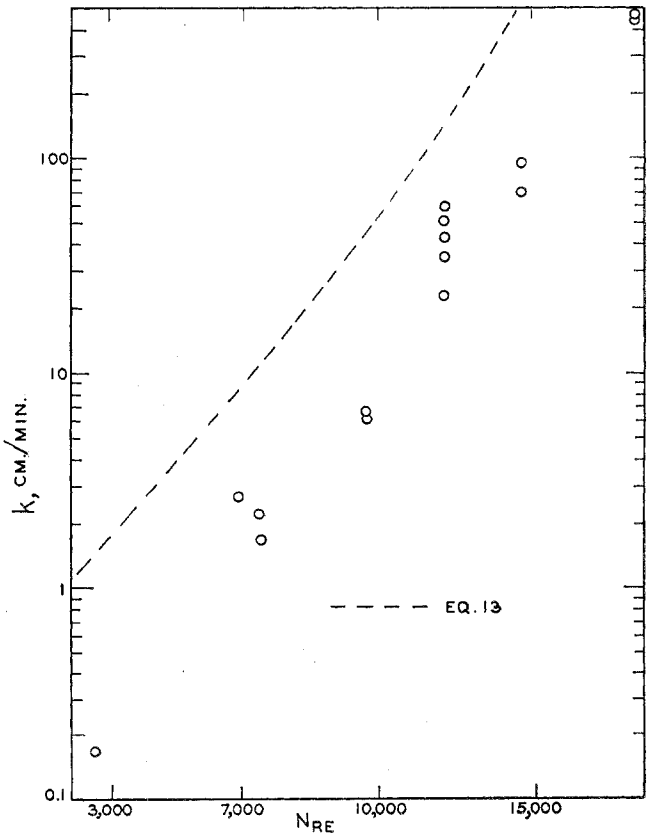

Figure 1. Deposition of 0.8-micron iron particles in 0.54-cm. glass tube

Table II. Ranges of Particle Sizes Counted

Nominal Size of Particles, Microns	Type of Particle	Size Range Counted, Microns
0.8	Iron	0.66 to 0.93
1.57	Iron	1.3 to 1.8
1.81	Iron	1.6 to 2.0
1.81	Aluminum	1.6 to 2.0
2.63	Iron	2.3 to 2.9

The iron particles were easy to size, as they were nearly all spherical and only a small percentage were present as agglomerates. The aluminum powder was more difficult to size because it contained spherical and oblong particles and a small percentage of flakes. Re-entrainment was encountered in the runs with the lycopodium spores at high air velocities, and only the runs at low velocity are reported. All of these were made in the 2.5-cm. brass tube with the glycerol jelly adhesive on the wall. At a velocity of 55 feet per second and with pressure-sensitive tape as the adhesive surface, no particles adhered to the surface.

Behavior of Particles at Wall

The deposition of the particles was followed under the microscope during several of the experiments. When re-entrainment was observed, either the adhesive or glycerol jelly was applied. The results obtained with the adhesives agree with those for the bare tube (Figures 1, 2, and 3); furthermore, results for the glass and brass tubes agree with one another. This indicates that rebounding was not important, as there is no reason to expect that the same fraction of particles would rebound from the different types of surfaces employed.

Re-entrainment of the 0.8-micron iron particles in the 0.54-cm. tube began at a Reynolds number of about 20,000; for the 1.57-micron iron particles in the 1.3-cm. tube at a Reynolds number of about 12,500. In general, the larger particles were more easily removed by the gas stream than the smaller ones. After passing the aerosol stream at a high velocity for a long time, the deposit consisted mostly of smaller particles, even though the rate of deposition increases with d_p^4. This agrees with the observation of Rumpf (*11*), who suggested that the larger particles are more easily removed from the wall since they project farther into the gas stream.

Mechanism of Particle Transport

In the absence of thermal gradients, four mechanisms may contribute to the transport of the suspended particles to the wall of a duct; gravitational, diffusional, electrostatic, and inertial forces. In the present work, gravitational effects were eliminated by making most of the runs in vertical tubes. Brownian diffusion was made negligible by using particles larger than 0.5 micron and high stream velocities. The agreement between the results obtained with glass and brass tubes indicates that electrostatic effects were of little significance. Thus, the most important transport mechanism appears to be the inertial effect of the eddies. Evidence of this is shown by the development of turbulence near the entrance to the tube. Two runs were made in which 0.8-micron particles were deposited from a stream passing through the 0.58-cm. glass tube, and the deposition rate was measured as a function of the distance from the inlet. With a bell-shaped inlet section, the velocity profile at the entrance is nearly uniform over the cross section. At the wall, however, the fluid is retarded and a boundary layer forms and continues to grow.

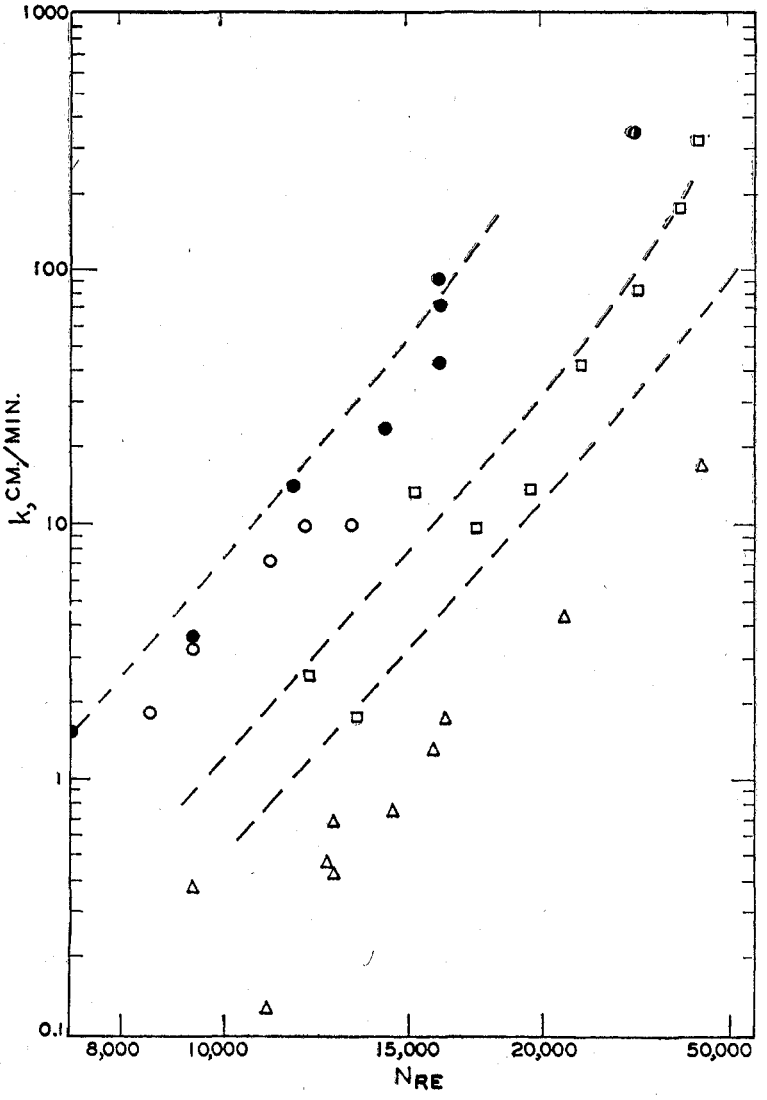

Figure 2. Deposition of iron and aluminum particles in glass and brass tubes of different sizes with different coatings

- ○. 1.57-micron iron particles, 1.30-cm. glass tube
- ●. 1.57-micron iron particles, 1.30-cm. glass tube, glycerol jelly adhesive
- ◑. 1.57-micron iron particles, 1.38-cm. brass tube, pressure-sensitive tape
- □. 1.81-micron aluminum particles, 1.38-cm. brass tube
- △. 0.8-micron iron particles, 1.30-cm. glass tube
- ———. Equation 13

If the Reynolds number based on duct diameter is greater than 2100, at some distance from the inlet the boundary layer becomes turbulent. The transition usually occurs at a Reynolds number based on distance from the entrance between 10^5 and 10^6, depending on the roughness of the wall and the level of turbulence in the main stream (*3*). If transport by eddies is important, the deposition rate near the entrance should follow the development of the turbulent boundary layer. Figure 4 shows the deposition rate as a function of distance from the inlet. No deposition occurs until N_{Re_x} is about 10^5;

the rate of deposition then approaches a constant value at $N_{Re_x} = 2 \times 10^5$ in the region of fully developed turbulence. The same effect was noted with the 1.38-cm. brass tube when two tests were made on the deposition at observation points located 34.8 and 53.7 diameters, respectively, from the inlet. With the exception of these tests, all measurements were made at points more than 26 diameters from the inlet.

Interpretation of Results

The experimental results are best interpreted by an analysis similar to that used by von Karman (*6*) for the rate of transport of momentum and mass in a turbulent gas stream. The shear stress is expressed by

$$\tau = (\mu + \rho\epsilon_g)\frac{dV}{dy} \qquad (1)$$

If it is assumed that the eddy diffusivities of mass and momentum are equal, the rate of mass transfer is

$$N = (D_v + \epsilon_g)\frac{dc}{dy} \qquad (2)$$

In the laminar sublayer, the eddy diffusivity is assumed to be zero. For the buffer region, ϵ_g can be obtained from the velocity profile; the Reynolds analogy is assumed to hold in the turbulent core. By integration of Equation 2 an equation is obtained for the mass transfer coefficient:

$$\frac{k}{V_{av}} = \frac{f/2}{1 + \sqrt{f/2}\left\{5(N_{Sc} - 1) + 5 \ln \frac{5N_{Sc} + 1}{6}\right\}} \qquad (3)$$

This analysis is satisfactory when the molecular diffusivity is approximately equal to the kinematic viscosity of the fluid—that is, when $N_{Sc} = 1$. For very large or very small values of the Schmidt number, however, von Karman's approach must be modified. Lin, Moulton, and Putnam (*9*) concluded that much of the transfer of dissolved substances of very low diffusivity is caused by the fluctuations in the laminar sublayer. Their data can be correlated if the eddy diffusivity in the sublayer is represented by

$$\epsilon_g = \nu\left(\frac{y^+}{14.5}\right)^3 \qquad (4)$$

The effect of small fluctuations in the sublayer on the transfer of momentum and on the velocity distribution is small; even at the edge of the sublayer where ϵ_g is at a maximum, it is only equal to $\nu/24.5$.

Eddy diffusion of particles suspended in a turbulent stream appears to be similar to the eddy diffusion of gas molecules, providing the particles are smaller than the scale of turbulence. Hence, it may be assumed that the eddy diffusivities of the particles and of the carrier gas are equal, although this has not been proved.

While the particles and fluid behave alike in the core of the turbulent fluid, they act differently near the wall. Gas molecules diffuse through the relatively stagnant layer to the surface, while particles with large inertia penetrate the quiescent region and reach the wall. On this basis, the following model is offered to explain the deposition of particles: Eddies carrying the particles diffuse from the turbulent core to within one stopping distance of the wall; this is the effective radius of the particles because of their inertia. It is the distance which a particle with a given initial velocity will move through a stagnant gas and is given by the equation

$$S = \frac{m}{K} v_{po} \qquad (5)$$

We shall assume that v_{po} is equal to the root mean square of the radial component of the fluctuating gas velocity, v_g'. (Actually, the mean particle velocity is probably less than the mean fluctuating gas velocity.) In the model suggested, S is an average distance, and no discontinuity in the concentration profile is envisioned.

Laufer (*8*) has measured v_g' at Reynolds numbers of 50,000 and 500,000 in a 10-inch duct. In the region near the wall, his data fall on a single curve when $v_g'/V_{av}\sqrt{f/2}$ is plotted against y^+; the group $v_g'/V_{av}\sqrt{f/2}$ increases from zero at the wall to about 0.9 at $y^+ = 80$ where its

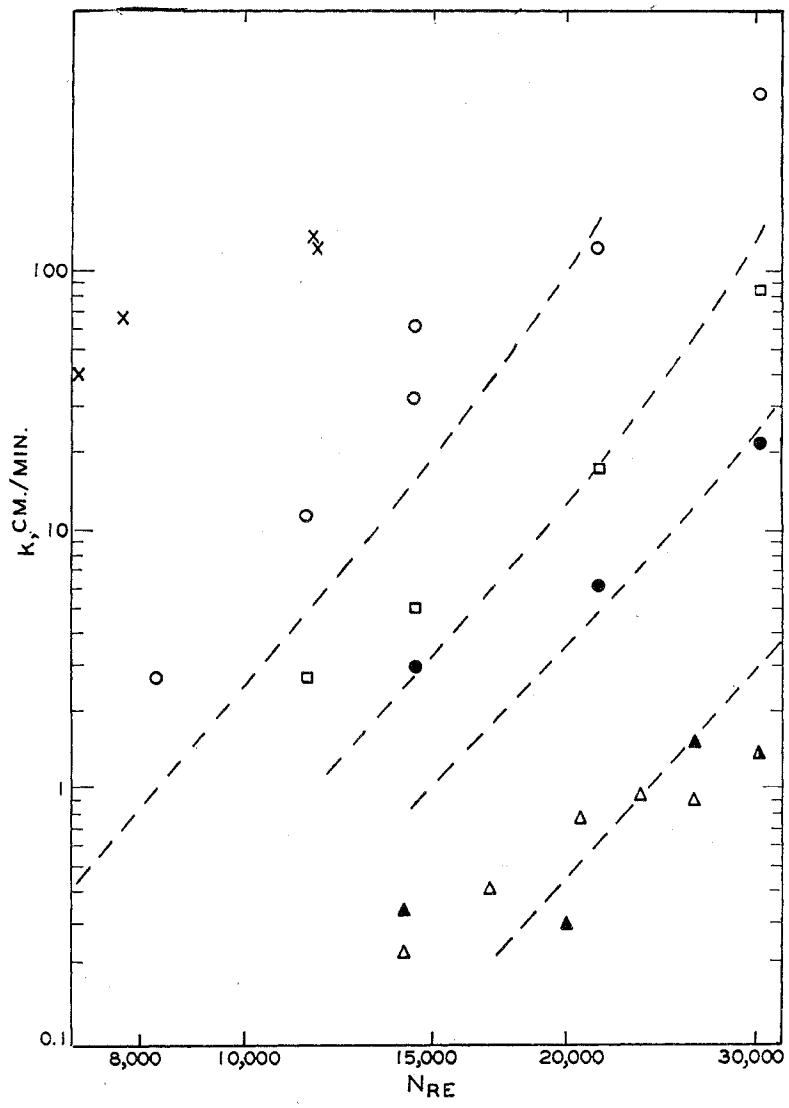

Figure 3. Deposition in 2.5-cm. glass and brass tubes

x. Lycopodium particles, 2.5-cm. brass tube, glycerol jelly adhesive
△. 0.8-micron iron particles, 2.5-cm. brass tube, pressure-sensitive tape
▲. 0.8-micron iron particles, 2.5-cm. glass tube
△. 0.8-micron iron particles, 2.5-cm. brass tube, pressure-sensitive tape
●. 1.32-micron iron particles, 2.5-cm. brass tube, pressure-sensitive tape
□. 1.81-micron iron particles, 2.5-cm. brass tube, pressure-sensitive tape
○. 2.63-micron iron particles, 2.5-cm. brass tube, pressure-sensitive tape
———. Equation 13

value becomes constant. In the analysis which follows, it is assumed that the particles come into the region near the wall with a velocity equal to 0.9 $V_{av}\sqrt{f/2}$, the mean fluctuating velocity of the gas just outside the buffer region. The stopping distances for each of the conditions studied were calculated on this basis. In nearly every case this distance was less than the thickness of the laminar sublayer, which is usually assumed to extend to $y^+ = 5$. The ratio of the calculated stopping distance to the thickness of the sublayer is shown in Figure 5. If there were no eddies in the laminar layer, no deposition would have occurred, because no particles would have diffused to within one stopping distance of the wall. Thus, it is necessary to assume that some fluctuations occur in the laminar sublayer. Lin, Moulton, and Putnam reached the same conclusion in their study of the transfer of materials of very low molecular diffusivity (*9*). For the particles used in the present work, the Stokes-Einstein diffusivity is negligible and the rate of transfer is

$$N = \epsilon_p \frac{dc}{dy} \tag{6}$$

If $\epsilon_p = \epsilon_g$, the rate of particle transfer through the sublayer is

$$N = \nu \left(\frac{y^+}{14.5}\right)^3 \frac{dc}{dy} \tag{7}$$

Since the particles need to diffuse only to one stopping distance from the wall, the limits of integration are $c = 0$ at $y^+ = S^+$, and $c = c_s$ at $y^+ = 5$. If N_0 is assumed to be constant through the sublayer,

$$c_s = \frac{(14.5)^3 N_0}{2V_{av}\sqrt{f/2}} \left[\frac{1}{S^{+2}} - \frac{1}{25}\right] \tag{8}$$

For the buffer layer, the eddy diffusivity is given by Lin, Moulton, and Putnam.

$$\frac{\epsilon_g}{\nu} = \frac{y^+}{5} - 0.959 \tag{9}$$

Substitution of this in Equation 7 and integration from $c = c_s$ at $y^+ = 5$ to $c = c_b$ at $y^+ = 30$, the edge of the turbulent core, gives

$$c_b - c_s = \frac{24\, N_0}{V_{av}\sqrt{f/2}} \tag{10}$$

In deriving Equation 10, N_0 is assumed to be constant through the buffer region.

The Reynolds analogy should hold in the turbulent core so that

$$c_{av} - c_b = \frac{N_0}{(f/2)V_{av}^2}(V_{av} - V_b) \tag{11}$$

Lin, Moulton, and Putnam (*9*) express the value of V_b by the equation

$$V_b = 13.73\, V_{av}\sqrt{f/2} \tag{12}$$

By adding Equations 8, 10, and 11 we obtain, after rearrangement and substitution,

$$\frac{k}{V_{av}} = \frac{f/2}{1 + \sqrt{f/2}\left(\frac{1525}{S^{+2}} - 50.6\right)} \tag{13}$$

This expression applies when S^+ is less than 5—that is, when the stopping distance is less than the thickness of the sublayer. The curves calculated from this equation are shown with the corresponding experimental values in Figures 1, 2, and 3. Table III shows the experimental data for the rate of deposition of iron particles and the calculated value of S^+. The deposition agrees with the predictions of the theory except in the case of the 0.8-micron particles, for which only the trend is consistent with the theory. The greatest uncertainty in the particle size was in these runs. Actually the calculated curve would agree closely with the experimental values if the particle diameter were 0.65 instead of 0.5 micron.

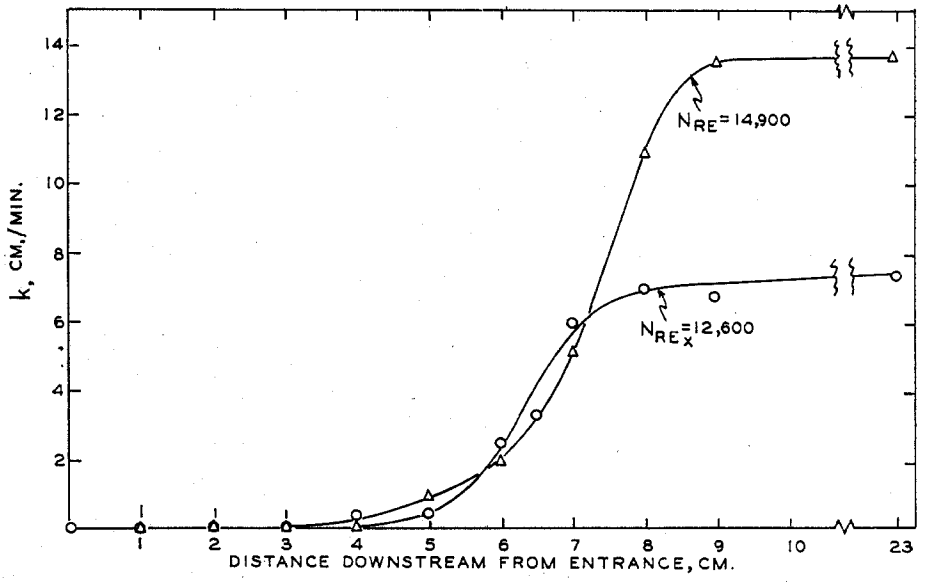

Figure 4. Deposition of 0.8-micron iron particles near entrance of 0.58-cm. tube

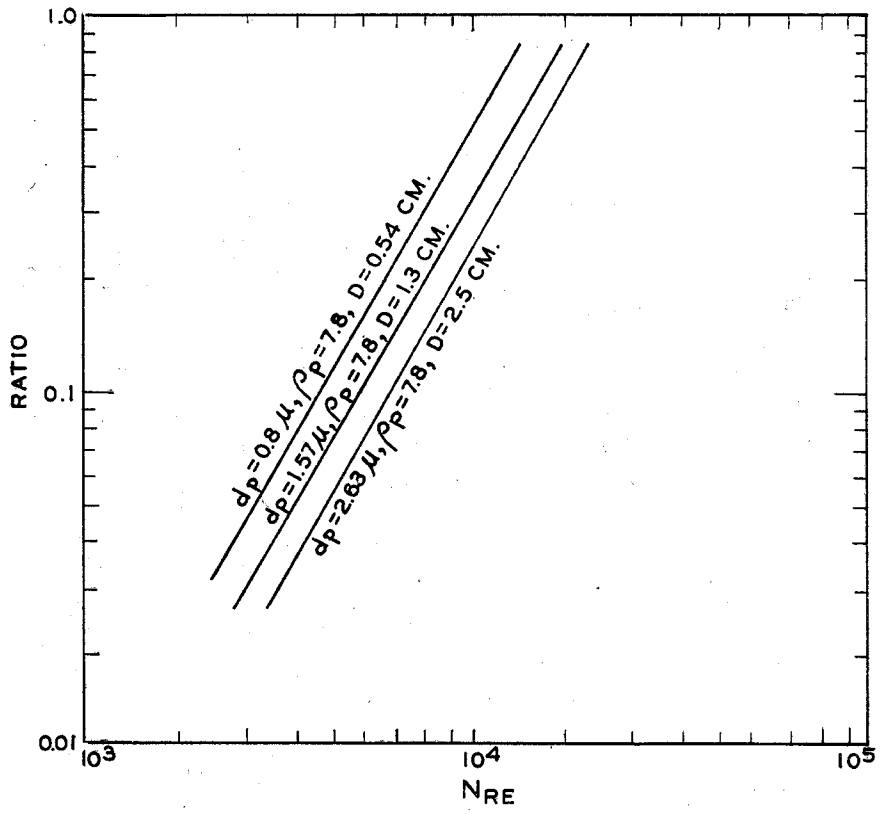

Figure 5. Ratio of stopping distance to thickness of laminar layer

Table III. Deposition of 0.8-Micron Iron Particles on Wall of 0.54-Cm. Glass Tube

Run	N_o, Particles/(Sq. Cm.)(Min.)	c_{av}, Particles/Cc.	k, Cm./Min.	V_{av}, Ft./Sec.	N_{Re}	S^+
0	13,900	8,300	1.67	67	7,450	1.50
3	46,900	7,680	6.1	87	9,700	2.38
4	58,500	8,920	6.64	87	9,700	2.38
6	43,300	18,850	2.29	67	7,450	1.48
7	33,200	1,440	23.1	106	11,900	3.44
9	33,300	660	50.3	106	11,900	3.44
11	37,800	630	59.8	106	11,900	3.44
12	36,900	1,060	34.9	106	11,900	3.44
13	0	29,900	0	27	3,000	...
14	5,100	29,900	0.17	43	4,800	0.67
15	66,500	1,510	44.1	107	11,950	3.45
16	39,500	14,900	2.65	62	6,950	1.32
17	61,900	900	69	131	14,600	4.96
19	15,800	170	95	131	14,600	4.96
20	19,400	42	460	180	19,400	8.33
21	24,500	55	445	180	19,400	8.33

When the stopping distance is small—i.e., when S^+ is less than about 1—Equation 13 reduces to

$$\frac{k}{V_{av}} = \sqrt{f/2}\,\frac{S^{+2}}{1525} = \frac{\rho^2 d_p^4 \rho_p^2 V_{av}^4}{6.1(10)^5\mu^4}\,(f/2)^{5/2} \quad (14)$$

This equation shows the extremely rapid increase of transfer rate with particle diameter and gas velocity when the stopping distance is less than the sublayer thickness.

If S^+ is between 5 and 30, the rate of transfer can be calculated by integration of Equation 6 between the limits $c = 0$ at $y^+ = S^+$ and $c = c_b$ at $y^+ = 30$, using the Reynolds analogy for the core. This gives finally:

$$\frac{k}{V_{av}} = \frac{f/2}{1 + \sqrt{f/2}\left\{5 \ln\left[\frac{5.04}{S^+/5 - 0.959}\right] - 13.73\right\}} \quad (15)$$

Only a few runs were made in this region. The data for the lycopodium powder shown in Figure 3 fall below the curve predicted by the theory.

No data were obtained for stopping distances greater than the combined thickness of the sublayer and buffer regions. In this range, the particles need to diffuse only to the edge of the buffer layer, so that the Reynolds analogy applies and

$$\frac{k}{V_{av}} = \frac{f}{2} \quad (16)$$

The suggested model predicts therefore that the rate of transfer of particles is always less than or, at most, equal to the rate of transfer of the common gases which follow approximately the Reynolds analogy.

Nomenclature

c = concentration, particles or moles per cc.
c_s = concentration at $y^+ = 5$, particles or moles per cc.
c_b = concentration at $y^+ = 30$, particles or moles per cc.
c_{av} = average concentration, particles or moles per cc.
d_p = particle diameter, cm.
D = tube diameter, cm.
D_c = scale of turbulence
D_v = molecular diffusivity of gas, sq. cm./second
f = friction factor, dimensionless
k = transfer coefficient, cm. per minute
k_c = transfer coefficient based on concentration at center of duct, cm. per minute
K = $3\pi\mu d_p$
L_t = distance from tube inlet to observation region, cm.
m = mass of particle
N = mass flux, particles or moles/(sq. cm.) (min.)
N_o = mass flux at wall, particles or moles/(sq. cm.) (min.)
N_{Re} = Reynolds number, $DV\rho/\mu$, dimensionless
N_{Re_x} = Reynolds number based on distance from tube entrance, dimensionless
N_{Sc} = Schmidt number, $\mu/\rho D_v$, dimensionless
S = stopping distance, cm.
S^+ = reduced stopping distance, $\frac{SV_{av}\rho}{\mu}\sqrt{f/2}$, dimensionless
v_g' = root mean square gas velocity, cm./sec.
v_p = particle velocity, cm. per second
v_{po} = velocity of particle at zero time, cm. per second
V = velocity of gas in axial direction at any point, cm. per second
V_{av} = average gas velocity, cm. per minute
V_b = gas velocity at $y^+ = 30$
y = distance from duct wall, cm.
y^+ = $\frac{y V_{av}\rho}{\mu}\sqrt{f/2}$, dimensionless
ϵ_g = eddy diffusivity of gas, sq. cm. per second
ϵ_p = eddy diffusivity of particle, sq. cm. per second
μ = gas viscosity, poises
$\nu = \mu/\rho$ = kinematic viscosity, sq. cm. per second
ρ = gas density, grams per cc.
ρ_p = particle density, grams per cc.
τ = shear stress, dynes per sq. cm.

Acknowledgment

This work is a part of the program on Contract No. AT(11-1)-276, in the Engineering Experiment Station, with the U. S. Atomic Energy Commission on a fundamental study of aerosols.

Literature Cited

(1) Alexander, L. G., Coldren, C. L., Ind. Eng. Chem. **43**, 1325 (1951).
(2) Friedlander, S. K., Ph.D. thesis, University of Illinois, 1954; *Univ. Microfilms* (Ann Arbor, Mich.), *Publ.* No. **10,476**, *Dissertation Abstr.* **15**, 95 (1955).
(3) Goldstein, S., "Modern Developments in Fluid Dynamics," vol. **I**, p. 326, Oxford University Press, London, 1938.
(4) Gregory, P. H., *Ann. Appl. Biol.* **38**, 357 (1951).
(5) Kalinske, A. A., van Driest, E. R., Proceedings of Fifth International Congress on Applied Mechanics, Cambridge Mass., p. 416, Wiley, New York, 1938.
(6) Karman, T. von, *Trans. Am. Soc. Mech. Engrs.* **61**, 705 (1939).
(7) Kohl, J., Zentner, R. D., *J. Phys. Chem.* **57**, 68 (1953).
(8) Laufer, J., Natl. Advisory Comm. Aeronaut., Tech. Note **2954** (1953).
(9) Lin, C. S., Moulton, R. W., Putnam, G. L., Ind. Eng. Chem. **45**, 636 (1953).
(10) Longwell, J. P., Weiss, M. A., *Ibid.*, **45**, 667 (1953).
(11) Rumpf, H., *Chem.-Ing.-Tech.* **6**, 317 (1953).
(12) Vanoni, V. A., Hsu, E. Y., Paper 67, centennial convocation, Am. Soc. Mech. Engrs., Chicago, 1952.

Received for review July 16, 1956
Accepted November 16, 1956

Division of Industrial and Engineering Chemistry, 130th Meeting, ACS, Atlantic City, N. J., September 1956.